Effector-mediated subversion of proteasome activator (PA)28αβ enhances lysosomal targeting of *Legionella pneumophila* within cytokine-activated macrophages

Tshegofatso Ngwaga[1], Deepika Chauhan[1], Abigail G. Salberg[1], and Stephanie R. Shames[1]*

[1]Division of Biology, Kansas State University, Manhattan, Kansas, 66506, USA

*Correspondence: sshames@ksu.edu

Address: 347 Ackert Hall, 1717 Claflin Road, Manhattan, Kansas, 66506 USA

Phone: (785) 532-0110

Keywords: PA28, proteasome, phagolysosomal fusion, cytokines, cell-autonomous immunity, *Legionella pneumophila*, LegC4, proteostasis, oxidative stress

Abstract

Legionella pneumophila is a natural pathogen of protozoa that causes Legionnaires' Disease pneumonia via replication within macrophages using hundreds of translocated effector proteins. In metazoans, effectors can also enhance pathogen clearance via effector-triggered immunity. The effector LegC4 confers a fitness disadvantage on *L. pneumophila* uniquely within cytokine-activated macrophages, but the mechanism is unknown. Here, we demonstrate that LegC4 restriction occurs via subversion of proteasome activator (PA)28αβ, which is induced by cytokines and functions to resolve oxidative stress. LegC4 impaired resolution of oxidative stress and LegC4-mediated restriction was abolished within PA28αβ-deficient macrophages. Impaired proteasome activity upregulates lysosomal degradation pathways and, indeed, subversion PA28αβ by LegC4 enhanced lysosomal fusion with the *Legionella*-containing vacuole. PA28αβ has been traditionally associated with antigen presentation; however, our data support a new model whereby subversion of PA28αβ enhances macrophage cell-autonomous immunity against *L. pneumophila*. This work provides a solid foundation to evaluate induced proteasome regulators as mediators of innate immunity.

32 **Introduction**

33 Many intracellular bacterial pathogens cause disease by replicating within host macrophages
34 (Mitchell et al., 2016). However, macrophages activated by T_H1 proinflammatory cytokines, such
35 as tumor necrosis factor (TNF) and interferon (IFN)-γ, are potently and broadly microbicidal. Ac-
36 tivated macrophages are in a state of altered protein homeostasis (proteostasis), owing in part to
37 robust production of reactive oxygen species (ROS), which cause collateral damage to cellular
38 proteins. To cope with oxidative stress, cytokine signaling induces expression of proteasome acti-
39 vator (PA)28αβ, which engages proteolytic 20S proteasome core particles (CPs) and facilitates
40 degradation of oxidant-damaged proteins (Pickering et al., 2010). Impaired proteasome activity
41 causes compensatory upregulation of lysosomal degradation pathways, which are central to cell-
42 autonomous immunity within activated macrophages (Dikic, 2016). PA28αβ has been tradition-
43 ally associated with antigen presentation and adaptive immunity (Graaf et al., 2011; Preckel et al.,
44 1999); however, the contribution of PA28αβ to antimicrobial innate host defense has not been
45 investigated.

46

47 *Legionella pneumophila* is a natural pathogen of amoebae and the etiological agent of Legion-
48 naires' Disease, a severe inflammatory pneumonia of the elderly and immunocompromised that
49 results from uncontrolled bacterial replication within alveolar macrophages. *L. pneumophila* rep-
50 lication within macrophages has resulted from extensive co-evolution with their protozoan hosts
51 (Gomez-Valero et al., 2019; Hugoson et al., 2022; Park et al., 2020). To establish its intracellular
52 niche, the *Legionella*-containing vacuole (LCV), *L. pneumophila* employs hundreds of virulence
53 factors, called effector proteins, that are translocated into infected host cells by a Dot/Icm type IV
54 secretion system (T4SS) (Chauhan and Shames, 2021). Effectors are essential for virulence, but
55 their activity can also trigger upregulation of pro-inflammatory cytokines by infected macro-
56 phages via effector-triggered immunity (ETI) (Asrat et al., 2014; Fischer et al., 2019; Fontana et
57 al., 2011; Ngwaga et al., 2021). Pro-inflammatory cytokines are central to clearance of *L.*

58 *pneumophila* by healthy hosts, since they activate and potentiate the antimicrobial capacity of
59 infected macrophages. Inability to thwart innate host defenses is likely due to the rarity of *L. pneu-*
60 *mophila* transmission from person-to-person and consequent lack of selective pressure from the
61 mammalian immune system. Thus, *L. pneumophila* serves as a well-established model pathogen
62 to study mechanisms of antimicrobial innate immunity.
63
64 We discovered that the Dot/Icm-translocated effector LegC4 confers a fitness disadvantage on *L.*
65 *pneumophila* in a mouse model of Legionnaires' Disease (Shames et al., 2017). The *in vivo* LegC4
66 restriction phenotype is likely due to elevated levels of pro-inflammatory cytokines in the *L. pneu-*
67 *mophila*-infected lung since LegC4 impairs *L. pneumophila* replication within cultured macro-
68 phages when activated with exogenous tumor necrosis factor (TNF) or interferon (IFN)-γ
69 (Ngwaga et al., 2019; Shames et al., 2017). We also found that overexpression of *legC4* from a
70 complementing plasmid is sufficient to attenuate *L. pneumophila* replication within BMDMs that
71 produce TNF and signal through TNFR1 (Ngwaga et al., 2019). The evolutionary basis for reten-
72 tion of LegC4 by *L. pneumophila* stems from its importance for replication within its natural host,
73 *Acanthamoeba castellanii* (Shames et al., 2017). Thus, LegC4 confers quantifiable opposing phe-
74 notypes in natural (protozoa) and 'accidental' (mammalian) hosts, which is noteworthy since the
75 majority of *L. pneumophila* effectors are functionally redundant in laboratory models and have
76 no obvious growth phenotypes (Ghosh and O'Connor, 2017; Shames et al., 2017). The specific
77 augmentation of cytokine-mediated restriction by LegC4 represents a potentially novel mode of
78 ETI; however, the mechanism by which LegC4 functions and enhances cytokine-mediated re-
79 striction of *L. pneumophila* is unknown.
80
81 Here, we investigated the mechanism of LegC4 function within macrophages. We found that
82 LegC4 interacts with host PA28α and that the LegC4 restriction phenotype is abolished in PA28αβ
83 complex deficient (*Psme1/2*$^{-/-}$) bone marrow-derived macrophages. LegC4 also suppressed

84 resolution of oxidative stress and enhanced lysosomal fusion with *Legionella*-containing vacuoles
85 (LCVs) in a cytokine- and PA28αβ-dependent manner. Overall, our data support a model whereby
86 PA28α targeting by a translocated effector protein perturbs proteostasis and enhances cell-au-
87 tonomous restriction of *L. pneumophila* within cytokine-activated macrophages. These data are
88 the first to define a role for PA28αβ in cell-autonomous host defense against an intracellular bac-
89 terial pathogen and reveal a mechanism by which to enhance the antimicrobial activity of acti-
90 vated macrophages.
91
92 **Results**
93 **LegC4 enhances restriction of *L. pneumophila* within cytokine-activated macro-**
94 **phages and *in vivo*.** We previously reported that LegC4 confers a fitness disadvantage on *L.*
95 *pneumophila* in intranasal C57Bl/6 mouse models of Legionnaires' Disease (LD) and within cy-
96 tokine-activated macrophages (Ngwaga et al., 2019; Shames et al., 2017). C57Bl/6 mice are re-
97 strictive to *L. pneumophila* due to flagellin (FlaA)-mediated activation of the NAIP5/NLRC4 in-
98 flammasome (Molofsky et al., 2006; Ren et al., 2006). Thus, to study FlaA-independent host re-
99 sponses within C57Bl/6 mice, we leverage FlaA-deficient *L. pneumophila* (Δ*flaA*) strains. Using
100 competitive index experiments, we found that *L. pneumophila* Δ*flaA*Δ*legC4* (herein called ΔΔ)
101 mutant strains outcompeted parental Δ*flaA* strains in the lungs of C57Bl/6 wild-type (WT) mice
102 (Ngwaga et al., 2019). The fitness advantage associated with loss of legC4 is likely due to enhanced
103 levels of cytokines seen in the *L. pneumophila*-infected lung compared to cultured macrophages
104 (Liu et al., 2020) since the LegC4-mediated fitness defect was phenocopied within macrophages
105 activated with exogenous recombinant (r)TNF or rIFN-γ (Ngwaga et al., 2019). We also found that
106 LegC4-mediated restriction can be observed in non-cytokine activated (naïve) BMDMs by over-
107 expressing *legC4* from an inducible promoter on a complementing plasmid (Ngwaga et al., 2019).
108 Thus, LegC4 is deleterious to *L. pneumophila* in a dose-dependent manner within cytokine-acti-
109 vated macrophages. The LegC4 restriction phenotype is not exclusive to mouse macrophages

110 since LegC4 confers a comparable fitness disadvantage on *L. pneumophila* within human THP-1
111 macrophages (**Fig 1A-B**). Further support and utility of the LegC4 overexpression model was ev-
112 idenced by loss of LegC4-mediated restriction within BMDMs unable to produce or respond to
113 endogenous TNF (*Myd88*$^{-/-}$ and *Tnfr1*$^{-/-}$, respectively) (**Fig 1C, 1D**) (Ngwaga et al., 2019). IFN-γ
114 signaling is sufficient for LegC4 restriction (Ngwaga et al., 2019); however, the LegC4 restriction
115 phenotype was retained within *Ifngr1*$^{-/-}$ BMDMs (**Fig 1E**), indicating that the relatively low levels
116 of IFN-γ secreted by macrophages are not sufficient for restriction.

117 We subsequently evaluated how cytokine signaling impacts the fitness of LegC4-deficient
118 bacteria *in vivo*. We confirmed our previous results showing that LegC4 is deleterious to *L. pneu-*
119 *mophila* within the lungs of WT and TNFR1-deficient mice (**Fig 1F**). We also found that LegC4
120 still conferred a fitness disadvantage on *L. pneumophila* within the lungs of MyD88- and IFNGR1-
121 deficient mice (**Fig 1F**). However, the fitness advantage associated with loss of LegC4 was less
122 pronounced in the lungs of *Myd88*$^{-/-}$ mice compared to WT, *Tnfr1*$^{-/-}$ and *Ifngr1*$^{-/-}$ (**Fig 1F**), which
123 is mainly due to the relatively low levels of MyD88-indpendent IFN-γ produced in the *L. pneu-*
124 *mophila*-infected lung (Archer and Roy, 2006). These data support our previous work showing
125 that LegC4 augments redundant cytokine-mediated pathogen restriction mechanisms (Ngwaga
126 et al., 2019) and demonstrate relevance to human cells. While overexpression of *legC4* is not nec-
127 essary to observe a phenotype (Ngwaga et al., 2019), this infection model is robust and useful for
128 our goal to define LegC4 function and mechanisms of cytokine-mediated restriction within mac-
129 rophages.

130

131 **LegC4 interacts with host proteasome activator (PA)28α**. To gain insight into the mech-
132 anism of LegC4 function, we conducted a yeast two-hybrid (Y2H) interactomics screen using
133 LegC4 as bait and genomic (g)DNA from mouse splenocytes as prey. This screen revealed inter-
134 actions between LegC4 and several regulators of eukaryotic proteasomes, including proteasome
135 activator (PA)28α, PA28γ, and Ecm29 (**Table S1**). The highest-confidence interactor was PA28α

136 with 28 individual clones, all of which encoded a minimal overlapping region in the PA28α C-
137 terminal domain (amino acid residues 105-249) (**Table S1**). These data suggest a direct interac-
138 tion between LegC4 and host PA28α, which is conserved in amoebae and induced by cytokines in
139 macrophages.

140 We initially validated the PA28α-LegC4 interaction by reciprocal co-immunoprecipitation
141 and immunofluorescence microscopy on ectopically produced epitope tagged fusion proteins. Ec-
142 topic expression of PA28α was necessary in these experiments since it is expressed only in re-
143 sponse to cytokine signaling (Fabunmi et al., 2001; Seifert et al., 2010). We found that PA28α-
144 Myc co-immunoprecipitated with 3xFLAG-LegC4 (**Fig 2A**) and that 3xFLAG-LegC4 co-immuno-
145 precipitated with GFP-PA28α (**Fig 2B**). We also found that ectopically produced 3xFLAG-LegC4
146 co-localized with GFP-PA28α within transfected HeLa cells (**Fig 2C**). Furthermore, LegC4 influ-
147 enced GFP-PA28α localization since GFP-PA28α localized to the cell nucleus in the absence of
148 LegC4 **(Fig 2C-D**) (Soza et al., 1997). Finally, we quantified co-localization by calculating Pearson
149 Correlation Coefficients (PCC). PCC values indicated a significant positive correlation between
150 LegC4 and PA28α (PCC = 0.768 ± 0.028) compared to the GFP control (PCC = 0.468 ± 0.172)
151 (**Fig 2E**). Together, these data show that LegC4 interacts with host PA28α, which has not been
152 previously identified as a target of bacterial effectors.
153

154 **LegC4-mediated restriction of *L. pneumophila* is abolished in PA28αβ-deficient**
155 **BMDMs.** Based on the interaction between PA28α and LegC4, we tested the hypothesis that
156 PA28α is important for LegC4-mediated restriction of *L. pneumophila* within BMDMs. PA28α-
157 deficient (*Psme1*$^{-/-}$) mice are not commercially available, so we evaluated the role of PA28α using
158 BMDMs derived from PA28αβ-deficient (*Psme1/2*$^{-/-}$) mice (Preckel et al., 1999). PA28α associates
159 with PA28β to form the PA28αβ (11S) proteasome regulator (Mott et al., 1994). PA28β is homol-
160 ogous to PA28α but is dependent on PA28α for activity and is hypothesized to enhance the

161 interaction of PA28α with 20S proteolytic proteasome core particles (CPs) (Wilk et al., 2000). We
162 found that PA28αβ was necessary for LegC4-mediated restriction of *L. pneumophila* since the no
163 growth attenuation was associated with *legC4* overexpression compared to control strains within
164 *Psme1/2*$^{-/-}$ BMDMs (**Fig 2F**). Thus, our data suggest that PA28αβ activity is important for LegC4-
165 mediated restriction and support a model whereby LegC4 binds and regulates the function of
166 PA28α.
167
168 **LegC4 impairs resolution of oxidative proteotoxic stress.** In cells of the innate immune
169 system, PA28αβ is produced in response to oxidative stress, TNF, or IFN-γ (Fabunmi et al., 2001;
170 Hallermalm et al., 2001; Mott et al., 1994; Pickering et al., 2010), which provides an explanation
171 as to why LegC4 confers a growth phenotype within cytokine-activated cells. Induced PA28ab
172 associates with proteasome core particles (CPs) to generate antigenic peptides and resolve oxida-
173 tive stress by facilitating ubiquitin-independent proteasomal degradation of oxidant-damaged
174 (carbonylated) proteins (Graaf et al., 2011; Li et al., 2010). Since LegC4 binds PA28α and the
175 LegC4 restriction phenotype was dependent on PA28αβ (see **Fig 2F**), we hypothesized that LegC4
176 regulates PA28αβ activity.
177 Our yeast two-hybrid data suggest that LegC4 binds the CTD of PA28α, which is involved
178 in PA28αβ docking on proteolytic proteasome core particles and consequent proteasomal degra-
179 dation of oxidant damaged (carbonylated) proteins. We rationalized that LegC4-meditated inhi-
180 bition of PA28αβ activity would impair degradation of carbonylated proteins and tested this by
181 quantifying protein carbonyls within macrophages. We first tested this within uninfected RAW
182 264.7 cells stably producing 3xFLAG-LegC4 (RAW-LegC4). Stable production of 3xFLAG-LegC4
183 was confirmed by confocal microscopy (**Fig 3A**) and Western blot (**Fig 3B**). Immunoprecipita-
184 tion was necessary to visualize LegC4 since it is produced by macrophages at low abundance.
185 However, this amount of ectopically produced LegC4 was sufficient to attenuate *L. pneumophila*

186 Δ*flaA* replication when compared to vector-transfected control (RAW-Cntrl) cells (**Fig 3C**). At-
187 tenuated growth was observed at 48 h post-infection, similar to the kinetics of LegC4 restriction
188 within BMDMs (**Fig 1A**), which suggests that RAW-LegC4 cells are suitable to evaluate whether
189 LegC4 impacts the concentration of carbonylated proteins within macrophages under oxidative
190 stress conditions.

191 We quantified the abundance of carbonylated proteins within lysates of uninfected RAW-
192 LegC4 and -Cntrl cells in the presence or absence H_2O_2 to induce oxidative stress. Under native
193 conditions, the concentration of carbonylated proteins within RAW-LegC4 and -Cntrl cells did
194 not differ (**Fig 3D**). However, under oxidative stress conditions, the concentration of protein car-
195 bonyls in RAW-LegC4 cells was significantly greater than control cells (**Fig 3D**). These data sug-
196 gest that cells producing LegC4 are impaired for resolution of oxidative proteotoxic stress and
197 support a model whereby LegC4 impairs PA28α activity.

198

199 **Oxidative stress is sufficient for LegC4-mediated restriction.** We subsequently evalu-
200 ated how LegC4 impacts the abundance of protein carbonyls within *L. pneumophila*-infected
201 cells. To control for differences in bacterial replication within WT BMDMs, we leveraged *Tnfr1*$^{-/-}$
202 BMDMs, in which LegC4 is not restrictive (see **Fig 1C**). *Tnfr1*$^{-/-}$ BMDMs were infected for 4 h in
203 the presence or absence of H_2O_2 and protein carbonyls were visualized by Western blot. We found
204 that the abundance of carbonylated proteins was increased within H_2O_2-treated BMDMs infected
205 with *L. pneumophila* Δ*flaA*Δ*legC4* (p*legC4*) relative to Δ*flaA* and empty vector control strains
206 (**Fig 3E**). Since no LegC4-mediated differences were observed within untreated *Tnfr1*$^{-/-}$, it is un-
207 likely that the increase in protein carbonyls observed is due to a LegC4-mediated upregulation
208 global ROS production by infected BMDMs. Together, these data support our hypothesis that
209 LegC4 impairs resolution of oxidative proteotoxic stress within macrophages.

210 Based on our data showing that LegC4 impairs resolution of oxidative proteotoxic stress,
211 we hypothesized that oxidative stress is sufficient for LegC4-mediated restriction within BMDMs.

212 To test this hypothesis, we quantified *L. pneumophila* replication within *Tnfr1*$^{-/-}$ BMDMs in the
213 presence or absence of H_2O_2 to induce oxidative stress. We found that replication of the *L. pneu-*
214 *mophila* Δ*flaA*Δ*legC4* (p*legC4*) strain was significantly attenuated within H_2O_2-treated *Tnfr1*$^{-/-}$
215 BMDMs compared to *L. pneumophila* Δ*flaA* and Δ*flaA*Δ*legC4* empty vector (pEV) control strains
216 (**Fig 3F**). These differences represent a 78% decrease in colony forming units (CFU), which is
217 striking since experimental limitations necessitated a low concentration (10 μM) of H_2O_2. It is
218 unlikely that growth attenuation was due to direct *L. pneumophila* killing by H_2O_2 since (1) repli-
219 cation of control *L. pneumophila* strains did not differ between H2O2-treated and untreated
220 BMDMs; and (2) *L. pneumophila* has evolved multiple complimentary strategies to protect
221 against oxidative stress and can withstand up to 2 mM H_2O_2 *in vitro* (orders of magnitude greater
222 than intracellular concentrations) (Bandyopadhyay and Steinman, 2000; Bandyopadhyay et al.,
223 2003; Flynn and Swanson, 2014; Harada et al., 2007). These data suggest that oxidative stress is
224 sufficient for the LegC4 restriction phenotype.
225
226 **PA28αβ-deficient BMDMs are restrictive to *L. pneumophila*.** Our current data suggest
227 that LegC4 binding impairs PA28αβ activity. Thus, we hypothesized that LegC4-mediated re-
228 striction of *L. pneumophila* would be phenocopied in PA28αβ-deficient BMDMs. To test this hy-
229 pothesis, we infected WT or *Psme1/2*$^{-/-}$ BMDMs with *L. pneumophila* Δ*flaA* in the presence or
230 absence of rTNF or rIFN-γ. We found that replication of *L. pneumophila* Δ*flaA* was significantly
231 attenuated within *Psme1/2*$^{-/-}$ BMDMs compared to WT BMDMs (**Fig 3G**). However, when
232 BMDMs were treated with either rTNF or rIFN-g, impaired bacterial replication was observed
233 within 24 h of infection whereas restriction was observed after 48 h in untreated BMDMs (**Fig**
234 **3H-I**). These data show that loss of PA28αβ enhances macrophage restriction of *L. pneumophila,*
235 which is more pronounced under inflammatory conditions and suggest a novel role for PA28αβ
236 in antimicrobial innate immunity.

237

238 **Neither PA28αβ nor LegC4 increase TNF secretion from *L. pneumophila*-infected**
239 **BMDMs or induce cell death.** We then evaluated whether differences in cytokine secretion or
240 cell death account for differences in PA28αβ- or LegC4-mediated restriction of *L. pneumophila*
241 within *Psme1/2*$^{-/-}$ compared to WT BMDMs. Autocrine and paracrine TNF signaling within *L.*
242 *pneumophila*-infected BMDMs is sufficient for the LegC4 restriction phenotype (Ngwaga et al.,
243 2019) (see **Fig 1D**); thus, we tested whether growth differences were due to increased TNF secre-
244 tion by infected BMDMs. At 8h post-infection, there were no differences in TNF secretion from
245 *Psme1/2*$^{-/-}$ BMDMs compared WT BMDMs infected with either *L. pneumophila* Δ*flaA* or ΔΔ
246 (pEV); however, there was less TNF secreted from *Psme1/2*$^{-/-}$ BMDMs infected with *L. pneu-*
247 *mophila* ΔΔ (p*legC4*) compared to WT BMDMs (**Fig S1A**). However, at 24 h post-infection, there
248 was significantly less TNF secreted from *Psme1/2*$^{-/-}$ BMDMs infected with *L. pneumophila* Δ*flaA*
249 or ΔΔ (pEV) compared to WT BMDMs but no differences in secretion from BMDMs infected with
250 *L. pneumophila* ΔΔ (p*legC4*) (**Fig S1B**). These data suggest that LegC4- and PA28αβ-mediated
251 growth phenotypes are not due to enhanced TNF production by infected BMDMs.

252 We subsequently evaluated whether LegC4 or PA28αβ affect viability of *L. pneumophila*-
253 infected BMDMs using lactate dehydrogenase release (LDH) assay. We found no LegC4- or
254 PA28αβ-mediated differences in LDH release from *L. pneumophila*-infected BMDMs (**Fig S1C**).
255 These data suggest neither LegC4 nor PA28αβ restriction phenotypes are a consequence of host
256 cell death.

257

258 **Phagolysosomal fusion contributes to LegC4-mediated restriction within BMDMs.**
259 Our current data suggest that LegC4 may impair PA28αβ activity, but how this leads to bacterial
260 restriction is unknown. Loss of cellular proteasome activity causes compensatory upregulation of
261 lysosomal degradation pathways to cope with proteotoxic stress (Dikic, 2016; Pandey et al., 2007).

262 Based on our data showing that oxidative proteotoxic stress is sustained in LegC4-producing cells,
263 we tested the hypothesis that LegC4 restriction involves lysosomal targeting of *L. pneumophila*.
264 Virulent *L. pneumophila* establish a replicative *Legionella*-containing vacuole (LCV) by blocking
265 endocytic maturation of their phagosome (Roy et al., 1998; Swanson and Isberg, 1995). However,
266 avirulent Dot/Icm-deficient *L. pneumophila* (Δ*dotA*) are unable to establish a replicative LCV and
267 phagosomes rapidly undergo endocytic maturation, as evidenced by localization of the lysosomal
268 membrane marker LAMP1 to *L. pneumophila*-containing phagosomes (Roy et al., 1998) (**Fig S2**).
269 We initially tested the hypothesis that LegC4 increases LAMP1 localization to LCVs by immuno-
270 fluorescence microscopy and blinded quantification of LAMP1$^+$ LCVs. As expected, there were
271 significantly fewer LAMP1$^+$ LCVs harboring Δ*flaA* and empty vector control strains compared to
272 the avirulent control within WT BMDMs (**Fig 4A**). However, there were no differences in the
273 percentage of LAMP1$^+$ LCVs harboring the ΔΔ (p*legC4*) strain compared to the Δ*dotA* control (**Fig**
274 **4A**), which was surprising since plasmid expression of *legC4* does not usually impair *L. pneu-*
275 *mophila* intracellular replication until after 24 h of infection. We found that LCVs harboring *L.*
276 *pneumophila* ΔΔ (p*legC4*) had significantly less LAMP1 staining compared to the Δ*dotA* strain
277 within both TNFR1- and PA28αβ-deficient BMDMs (**Fig 4B-C**). These data suggest that LegC4
278 upregulates lysosomal fusion with LCVs in a cytokine- and PA28αβ-dependent manner.

279 We subsequently tested the hypothesis that phagolysosomal fusion is important for
280 LegC4-mediated restriction by quantifying *L. pneumophila* replication within BMDMs treated
281 with Bafilomycin A1 (BAF). BAF is a pharmacological inhibitor of the H$^+$-type vacuolar (v)-ATPase
282 that blocks vacuolar acidification and impairs phagolysosomal fusion (Matsumoto and Nakanishi-
283 Matsui, 2019). Thus, we evaluated the contribution of phagolysosomal fusion to the LegC4 re-
284 striction phenotype by quantifying *L. pneumophila* replication within BAF-treated BMDMs. LCV
285 acidification is important for late stages of the *L. pneumophila* lifecycle (Sturgill-Koszycki and
286 Swanson, 2000); however, intracellular replication is minimally impacted within BMDMs treated
287 with a low concentration (≤12.5 nM) of BAF (Khweek et al., 2013). We found that replication of

288 *L. pneumophila* ΔΔ (p*legC4*) was not attenuated compared to *L. pneumophila* Δ*flaA* and ΔΔ
289 (pEV) strains within BAF-treated BMDMs (**Fig 4D, left**). As expected, *L. pneumophila* ΔΔ
290 (p*legC4*) replication was significantly attenuated compared to Δ*flaA* and ΔΔ (pEV) within vehicle
291 (DMSO)-treated BMDMs (**Fig 4D, right**). These data suggest a role for phagolysosomal fusion
292 and/or lysosomal acidification contribute to LegC4-mediated restriction. Together, our data sup-
293 port a model whereby LegC4-mediated subversion of PA28αβ enhances lysosomal pathogen tar-
294 geting within activated macrophages.
295
296 **Inflammasome activation is dispensable for LegC4-mediated restriction.** Our current
297 data suggest that LegC4-mediated restriction occurs via lysosomal fusion with LCVs under oxida-
298 tive proteotoxic stress conditions. However, sustained oxidative stress and proteostasis perturba-
299 tions can activate the NLRP3 inflammasome, which culminates in activation of caspase-1, an ef-
300 fector caspase responsible for pyroptotic cell death and inflammatory cytokine secretion. How-
301 ever, pharmacological inhibition of the NLRP3 inflammasome with MCC950 did not affect LegC4-
302 mediated restriction since *L. pneumophila* ΔΔ (p*legC4*) was still attenuated for replication com-
303 pared to *L. pneumophila* ΔΔ (pEV) and Δ*flaA* within WT BMDMs (**Fig S3A**). We also found that
304 LegC4-mediated restriction was preserved within BMDMs derived from caspase-1-deficient
305 (*Casp1*$^{-/-}$) mice (**Fig S3B**). Within cultured macrophages, pyroptotic cell death is responsible for
306 *L. pneumophila* restriction downstream of inflammasome activation. Our data suggest that LegC4
307 does not enhance LDH release from infected BMDMs (**Fig S3C**); however, pyroptotic cell death
308 is more pronounced within BMDMs primed with toll-like (TLR) receptor agonists (Bergsbaken et
309 al., 2009; Feuvre et al., 2002). Since TLR2 is important for host defense against *L. pneumophila*
310 (Archer and Roy, 2006), we evaluated LDH release from *L. pneumophila*-infected BMDMs pre-
311 treated with the TLR2 agonist PAM3CSK4. Consistent with our previous observation (**Fig S1C**),
312 LDH release from BMDMs primed with PAM3CSK4 was unaffected by LegC4 (**Fig S3C**). These

313 data suggest that LegC4-mediated restriction occurs independently of inflammasome activation
314 and pyroptotic cell death.
315
316 **Discussion**
317 This study supports a novel role for proteasome activator (PA)PA28αβ in effector-mediated host
318 defense against an intracellular bacterial pathogen. Our data show that LegC4 binds PA28αβ,
319 subverts resolution of oxidative proteotoxic stress and promotes lysosomal restriction of *L. pneu-*
320 *mophila*. Thus, we propose a model whereby prolonged oxidative proteotoxic stress resulting
321 from LegC4 subversion of PA28αβ enhances lysosomal targeting of *L. pneumophila* within cyto-
322 kine-activated macrophages (**Fig S4**). This model is supported by our data showing that (1) LegC4
323 binds PA28α; (2) PA28αβ is required for the effects of LegC4 on host cells; (3) LegC4 impairs
324 resolution of oxidative proteotoxic stress; and (4) that oxidative stress and phagolysosomal fusion
325 contribute to LegC4-mediated restriction of *L. pneumophila*. This work is the first describe
326 PA28α as a target for a bacterial effector protein and a role for PA28αβ in effector-mediated host
327 defense against an intracellular bacterial pathogen.
328
329 *L. pneumophila* is an accidental pathogen of humans that rarely transmits between infected indi-
330 viduals. Thus, an evolutionary basis for the LegC4- PA28α interaction can be explained by LegC4
331 targeting the PA28α homolog in amoebae. Indeed, the natural host *A. castellanii*, in which LegC4
332 is a *bona fide* virulence factor (Shames et al., 2017), encodes a PA28α homolog (*Ac*PA28) that
333 shares 34% identity with mouse PA28α. Sequence identity between PA28αβ and *Ac*PA28 is pri-
334 marily in the C-terminal domain, which is important for engaging 20S CPs and was contained in
335 all PA28α clones identified in our yeast two-hybrid screen (see **Table S1**). These data have led us
336 to speculate that LegC4 binding prevents PA28-CP complex formation. The function of *Ac*PA28
337 has not been described; however, structural studies have shown that mammalian PA28α and

338 evolutionary distant PA28s are similar and all associate with proteolytic proteasome core parti-
339 cles, suggesting that it likely also functions as a proteasome regulator (Lesne et al., 2020; Xie et
340 al., 2019). The constitutive 26S proteasome system is central to *L. pneumophila*'s virulence strat-
341 egy and its integrity may be preserved by sequestering PA28 from CPs. We are currently investi-
342 gating the molecular mechanism by which LegC4 regulates PA28 activity within macrophages and
343 amoebae and how this activity is advantageous to *L. pneumophila* in the natural host.
344
345 We found that inducing oxidative stress with hydrogen peroxide (H_2O_2) was sufficient for the
346 LegC4 restriction phenotype. H_2O_2 is routinely used to induce oxidative stress in laboratory mod-
347 els since both superoxide ($O_2^{\bullet-}$) and hydroxyl ($OH^{\bullet}$) radicals are highly reactive and unstable in
348 solution. Interestingly, reactive oxygen species (ROS) are important for *L. pneumophila* re-
349 striction by neutrophils but play a negligible role in macrophages (Harada et al., 2007; Price et
350 al., 2021; Ziltener et al., 2016). This difference has been attributed to suppression of global intra-
351 cellular ROS production and NADPH oxidase (NOX2) trafficking to the LCV by virulent *L. pneu-*
352 *mophila* within macrophages (Harada et al., 2007; Price et al., 2021). Direct oxidative killing of
353 *L. pneumophila* within activated macrophages is unlikely since *L. pneumophila* has evolved mul-
354 tiple complimentary strategies to protect against oxidative stress and can withstand up to 2 mM
355 H_2O_2 *in vitro* (orders of magnitude greater than intracellular concentrations) (Bandyopadhyay
356 and Steinman, 2000; Bandyopadhyay et al., 2003; Flynn and Swanson, 2014; Harada et al.,
357 2007). Moreover, *Tnfr1*$^{-/-}$ BMDMs treated with H_2O_2 did not suppress replication of *L. pneu-*
358 *mophila* control strains compared to untreated BMDMs (see Fig 3F). This suggests that the con-
359 centration of H_2O_2 used in our study is insufficient for direct *L. pneumophila* killing. Future stud-
360 ies will reveal whether LegC4 or PA28αβ impact the abundance or source of ROS within *L. pneu-*
361 *mophila*-infected macrophages.
362

363 Phagolysosomal fusion and autophagy are cytoprotective under inflammatory conditions and
364 central to cytokine-mediated cell-autonomous pathogen restriction. Lysosomal restriction within
365 IFN-γ-activated macrophages involves immunity-related GTPases (IRGs), which localize to and
366 facilitate lysosomal trafficking to pathogen-containing phagosomes (MacMicking, 2012). Alt-
367 hough IRGs may contribute to restriction of LegC4-producing *L. pneumophila* strains within IFN-
368 γ-activated macrophages (Naujoks et al., 2016), we found that IFNGR1 signaling is dispensable
369 for LegC4 restriction (Fig 1E), which suggests that IRGs are not central drivers of LegC4-mediated
370 *L. pneumophila* restriction. A role for TNFR1-mediated signaling in lysosomal pathogen re-
371 striction has not been well established. Canonically, TNF signaling activates extrinsic cell death
372 pathways; however, TNFR1-mediated signaling induces lysosomal fusion with LCVs within 3 h of
373 *L. pneumophila* infection within primary mouse BMDMs, which is more rapid compared to
374 BMDMs activated with IFN-γ (Ziltener et al., 2016).
375
376 The mechanism by which TNF signaling enhances phagolysosomal fusion with LCVs is poorly
377 understood; however, upregulation of autophagy genes is cytoprotective against TNF-induced
378 death in myeloid cells (Orvedahl et al., 2019). Autophagy is also upregulated to prevent aberrant
379 inflammasome-mediated pyroptotic cell death below a certain threshold of inflammasome ago-
380 nist (Byrne et al., 2013). The NLRC4 inflammasome is dispensable for LegC4-mediated restriction
381 (Ngwaga et al., 2019; Shames et al., 2017) and we also found no role for the NLRP3 inflam-
382 masome, which is activated by both oxidative and proteotoxic stress (Shin et al., 2013). Whether
383 autophagy contributes to LegC4-mediated restriction is unknown, but this possibility is intriguing
384 since several *L. pneumophila* effectors impair global autophagy in host cells (Choy et al., 2012;
385 Rolando et al., 2016b, 2016a).
386
387 Virulent *L. pneumophila* establish a replicative LCV by avoiding endosomal maturation of their
388 phagosome. The current dogma dictates that lysosomal fusion with LCVs at early time points

389 during infection (≤ 16 h) prevents *L. pneumophila* intracellular replication (Marra et al., 1992;
390 Sturgill-Koszycki and Swanson, 2000). We found that plasmid expression of *legC4* induced ro-
391 bust LAMP1 localization to LCVs within WT BMDMs, similar to what is seen for an avirulent a
392 Dot/Icm-deficient strain. This is intriguing since plasmid expression of *legC4* does not completely
393 abolish *L. pneumophila* intracellular replication (Ngwaga et al., 2019). Loss of TNFR1 did not fully
394 abolish LegC4-mediated LAMP1 localization to LCVs; however, this relatively modest level of
395 LAMP1 localization may result from ROS produced in response to pattern recognition receptors
396 (West et al., 2011). The abrogation of LegC4-mediated LAMP1-LCV localization within *Psme1/2*$^{-}$
397 $^{/-}$ supports our model that subversion of PA28αβ by LegC4 enhances lysosomal fusion with LCVs.
398
399 Here, we show a new role for PA28αβ and oxidative proteotoxic stress in cell-autonomous path-
400 ogen restriction. This work is the first to show bacterial pathogen targeting of PA28α and suggest
401 that suppression of PA28αβ activity and aberrant proteostasis may be a pathogen-triggered host
402 defense mechanism and mode of potentiating existing inflammatory responses. The ability en-
403 hance antimicrobial potential of activated macrophages has exciting implications for develop-
404 ment of host-centric innate immunological therapeutics and future studies will provide further
405 insight into the ubiquity and mechanism(s) of pathogen restriction induced by proteotoxic stress
406 and suppression of PA28αβ activity.
407
408 **Materials & Methods**
409 Bacterial Strains, Plasmids, and Culture conditions
410 *Legionella pneumophila* strains used in this study (**Table S2**) were cultured on supplemented
411 charcoal N-(2-Acetamido)-2-aminoethanesulfonic acid (ACES)-buffered yeast extract (CYE) and
412 grown at 37˚C as described (Feeley et al., 1979). Liquid cultures were grown overnight with shak-
413 ing at 37˚C in supplemented ACES-buffered yeast extract (AYE) medium, as described (Ngwaga
414 et al., 2019; Saito et al., 1981). For plasmid maintenance, CYE was supplemented with 10 μg mL^{-1}

415 chloramphenicol and *legC4* expression was induced with 1 mM isopropyl-β-D-1-thiogalactopyra-
416 noside (IPTG) where indicated. Plasmids used in this study are listed in **Table S3**. Oligonucleo-
417 tide primers are listed in **Table S4.**
418
419 Mice and bone marrow-derived macrophages
420 Wild-type, *Tnfr1*$^{-/-}$, *Ifngr1*$^{-/-}$, *Myd88*$^{-/-}$, and *Psme1/2*$^{-/-}$ on a C57BL/6 background were purchased
421 from the Jackson Laboratories (Bar Harbor, Maine) and in-house colonies were maintained in
422 specific pathogen-free conditions at Kansas State University. All experiments involving animals
423 were approved by the Kansas State University Institutional Animal Care and Use Committee (Pro-
424 tocols 4022, 4501, and 4386) and performed in compliance with the Animal Welfare Act and NIH
425 guidelines.
426 Bone marrow was harvested from seven- to twelve-week-old mice as described (Case and
427 Roy, 2013). BMDMs were generated by differentiation in RPMI supplemented with 20% heat-
428 inactivated fetal bovine serum (HI-FBS) (Biowest, Riverside, MO) and 15% L929 cell supernatant
429 for 6 days prior to seeding for infection. Femurs from C57Bl/6 *Casp1*$^{-/-}$ mice were a gift from Dr.
430 Russell Vance (University of California, Berkeley).
431
432 Competitive Index
433 Six- to twelve-week-old sex- and age-matched mice were infected as previously described. Mixed
434 bacterial inoculums (1:1) containing a total of 5 x 10^6 bacteria were diluted and plated on selective
435 medium (10 µg mL^{-1} chloramphenicol for plasmid selection). At 48 h post-infection, mice were
436 euthanized, and lung homogenates were plated on selective media as described (Ngwaga et al.,
437 2019). CFU were enumerated and used to calculate CI values
438 [$(CFUcm^R_{48h}/CFUwt_{48h})/(CFUcm^R_{IN})/CFUwt_{IN})$].
439
440 Molecular Cloning

441 Plasmids were generated for stable and transient ectopic production in mammalian cells. For pro-
442 duction of 3xFLAG-LegC4, *legC4* was amplified from *L. pneumophila* genomic (g)DNA using
443 LegC4BamHI-F/LegC4NotI-R primer pairs and cloned as a BamHI/NotI fragment into 3xFLAG
444 4/TO (Ingmundson et al., 2007). To produce GFP-PA28α, *psme1* was amplified from pCMV-
445 3Tag-4a::*psme1* (purchased from Genscript, Piscataway, New Jersey) using Psme1Sal1-
446 F/Psme1BamHI-R primer pairs and cloned as a Sal1/BamH1 fragment into pEGFPC1 (Clontech).
447 Plasmid DNA was transfected into mammalian cells as described below.
448
449 Cell Culture and Transfections
450 HEK 293T, HeLa, RAW 264.7 cells, and MH-S cells (gifts from Dr. Craig Roy, Yale University)
451 were maintained at 37˚C and 5% CO_2 in Dulbecco's Modified Eagle Medium (DMEM) supple-
452 mented with 10% HI-FBS. THP-1 cells were purchased from the American Type Culture Collection
453 (ATCC) and maintained in RPMI supplemented with 10% HIFBS and differentiated with 100 nM
454 phorbal 12-myristate 13-acetate (PMA) for 4 days prior to infection with *L. pneumophila* (see be-
455 low). All cell lines were used between passage 4-20.
456 HEK 293T cells were transfected with purified plasmid DNA (**Table S2**) using calcium
457 phosphate as described (Shames et al., 2010). Lysates were generated from transfected cells after
458 48 h and used for immunoprecipitation and Western blot analysis (see below). HeLa cells were
459 seeded one day prior to transfection with jetPRIME transfection reagent according to manufac-
460 turer's guidelines. Two hours before transfection, HeLa cells were washed and incubated in low-
461 serum media (DMEM 4% HIFBS. Media were replaced with DMEM 10% HIFBS four hours post-
462 transfection and assayed 24 h post-transfection.
463 To generate RAW 264.7 cells with stable plasmid integrations, cells were transfected with
464 pcDNA::*3xflag-legC4* or pcDNA::*3xflag* vector using a Nucleofector 2b electroporator (Lonza,
465 Basel, Switzerland) and cultured over 14 days with Zeocin selection for 14 days (200 -1000 μg mL^{-1}
466). Stable RAW 264.7 cells were maintained in culture in the presence of 200 μg mL^{-1} Zeocin. For

467 *L. pneumophila* infections, cells were seeded one day prior to infection in the absence of Zeocin.
468 Production of ectopic 3xFLAG-LegC4 was confirmed by Western blot and confocal microscopy
469 using α-FLAG antibodies (see below).
470
471 Western blot
472 Boiled protein samples were separated by SDS-PAGE and transferred to polyvinylidene difluoride
473 (PVDF) membrane using a BioRad TransBlot semidry transfer apparatus. Membranes were incu-
474 bated in blocking buffer [5% non-fat milk powder dissolved in Tris-buffered saline-0.1% Tween-
475 20 (TBST)]. Primary antibodies [rabbit α-FLAG (Sigma-Aldrich, F1804), rabbit α-Myc (Cell Sig-
476 naling, 2278S), rabbit α-GFP (Abcam, ab6556)] were used at 1:1,000 in blocking buffer and de-
477 tected with horseradish peroxidase (HRP)-conjugated secondary antibodies (1:5,000; Ther-
478 moFisher). Membranes were washed in TBST followed by addition of enhanced chemilumines-
479 cent (ECL) reagent (GE Amersham) and visualization using an Azure c300 Darkroom Replacer.
480
481 Immunoprecipitation
482 Transiently transfected HEK 293T cells or RAW 264.7 cells were washed with phosphate-buffered
483 saline and lysed in ice-cold NP-40 buffer [1% non-iodet P40 (v/v), 20 mM Tris pH 7.5, 150 mM
484 NaCl, 10 mM $Na_4P_2O_7$, 50 mM NaF, complete protease inhibitor (Roche)]. Lysates were clarified
485 and added to magnetic Protein G-conjugated Dynabeads that had been pre-incubated with either
486 mouse a-FLAG M2 antibody (Sigma Aldrich) or rabbit a-GFP antibody (Abcam, ab6556) accord-
487 ing to manufacturer's instructions. Input samples were collected from cell lysates prior to incuba-
488 tion with beads. Beads and input samples were resuspended in 3x Laemmli sample buffer for
489 Western blot analysis.
490
491 Protein carbonyl assays

492 Protein carbonyls were quantified using the OxiSelect™ Protein Carbonyl ELISA Kit (Cell Biolabs)
493 following manufacturer's instructions. Briefly, RAW 264.7 cells were seeded at $5x10^5$ in a 6-well
494 plate in DMEM 10% HIFBS. The next day, media were aspirated, and cells were incubated in
495 DMEM/2.5% HIFBS in the presence or absence of 10 μM H_2O_2. After 24 h, cells were washed
496 twice in PBS and lysed in ice-cold 500 μL of detergent-free lysis buffer [25 mM HEPES pH 7.4,
497 150 mM NaCl, 10 mM $MgCl_2$, 1 mM EDTA, 2% glycerol (v/v)] supplemented with complete pro-
498 tease inhibitor cocktail (Roche). Cell lysates were scraped into a pre-chilled microcentrifuge tube
499 and incubated with agitation for 30 min at 4˚C followed by sonication at 40% intensity three times
500 in 10 second intervals. Lysates were clarified by centrifugation at 4˚C for 20 min at 12,000 rpm.
501 Supernatants were transferred to a fresh tube, snap frozen in liquid nitrogen for 2 min and stored
502 at -80˚C until use. Protein concentrations were quantified using a Coomassie Plus (Bradford)
503 Protein Assay (Pierce) and diluted to 10 μg mL^{-1}. Samples and standards were adsorbed to a 96-
504 well protein binding plate and ELISA was performed according to manufacturer's instructions.
505 Absorbance at 450 nm was quantified on a BioTek Epoch2 microplate reader.

506 Protein carbonyls were visualized using the OxiSelect™ Protein Carbonyl Immunoblot Kit
507 (Cell Biolabs). *Tnrf1*$^{-/-}$ BMDMs were seeded in 24-well plates at $2.5x10^5$ one day prior to infection
508 with indicated *L. pneumophila* strains at an MOI of 50 in the presence or absence of 10 μM H_2O_2.
509 One hour after infection, cells were washed 3x with PBS$^{-/-}$, media were replaced and cells were
510 incubated for an additional 3 h in the presence or absence of H_2O_2. Cells were washed in ice-cold
511 PBS-/- and lysed in 120 μL ice-cold NP-40 lysis buffer (see above). Lysates were diluted in 3x
512 Laemmli sample buffer and boiled for 10 min. Proteins were separated on a 4-20% gradient SDS-
513 PAGE gel and transferred to PVDF membrane using a BioRad TransBlot semi-dry transfer appa-
514 ratus. Membranes were processed according to manufacturer's instructions using 10 min wash
515 steps. Blots were stripped and re-probed with rabbit a-b-actin antibody (1:1000; Cell Signaling
516 Technology) followed by goat-a-rabbit-HRP (1:5000; ThermoFisher). Blots were visualized as de-
517 scribed above and densitometry was performed using ImageJ.

518

519 Yeast Two-Hybrid Analysis

520 Yeast two-hybrid screening was performed by Hybrigenics Services, S.A.S., Evry, France
521 (http://www.hybrigenics-services.com). The *legC4* coding sequence was PCR-amplified from
522 pSN85::*legC4* (Ngwaga et al., 2019)and cloned into pB66 as a C-terminal fusion to Gal4 DNA-
523 binding domain (Gal4-C4). The construct was checked by sequencing and used as a bait to screen
524 a random-primed Mouse Spleen library constructed into pP6. pB66 derives from the original
525 pAS2ΔΔ vector (Fromont-Racine et al., 1997) and pP6 is based on the pGADGH plasmid (Bartel
526 and Fields, 1995).

527 Sixty million clones (6-fold the complexity of the library) were screened using a mating
528 approach with YHGX13 (Y187 ade2-101::loxP-kanMX-loxP, mat-α) and CG1945 (mat-a) yeast
529 strains as previously described (Fromont-Racine et al., 1997). 303 His+ colonies were selected on
530 a medium lacking tryptophan, leucine and histidine, and supplemented with 2mM 3-aminotria-
531 zole to handle bait autoactivation. The prey fragments of the positive clones were amplified by
532 PCR and sequenced at their 5' and 3' junctions. The resulting sequences were used to identify the
533 corresponding interacting proteins in the GenBank database (NCBI) using a fully automated pro-
534 cedure. A confidence score (PBS, for Predicted Biological Score) was attributed to each interaction
535 as previously described (Formstecher et al., 2005).

536

537 Immunofluorescence Microscopy

538 To quantify LAMP1-LCV co-localization and the number of *L. pneumophila* per LCV, $1x10^5$
539 BMDMs were seeded on poly-L-lysine-(PLL)coated glass coverslips in 24-well plates and infected
540 with *L. pneumophila* at a multiplicity of infection (MOI) of 30 in triplicates. Coverslips were fixed
541 with 4% paraformaldehyde (PFA; ThermoFisher) and permeabilized in ice cold methanol. Co-
542 verslips were incubated with 1:1,000 rabbit α-*L. pneumophila* (Invitrogen, PA17227), rat α-
543 LAMP1 (Developmental Studies Hybridoma Bank) primary antibodies and 1:500 Alexa 488-

544 conjugated goat α-rabbit and Alexa594-conjugated goat α-rat secondary antibodies (Ther-
545 moFisher) in blocking buffer [0.1% saponin (w/v), 1% HIFBS (v/v), 0.5% bovine serum albumin
546 (BSA; w/v)] in PBS. Nuclei were stained with Hoechst (ThermoFisher) at 1:2,000. Coverslips were
547 mounted on glass slides with ProLong Gold Antifade Mountant (ThermoFisher). LAMP1 localiza-
548 tion to LCVs were scored blind on a Leica DMiL LED inverted epifluorescence microscope (*n*=300
549 cells/strain).

550 For confocal microscopy, HeLa cells were seeded on PLL-coated coverslips and trans-
551 fected as described above. Coverslips were fixed in 4% PFA and processed as described above
552 using mouse α-FLAG M2 (Sigma; 1:1,000) and rabbit α-GFP (Abcam; ab6556; 1:5,000) primary
553 antibodies and Alexa546-conjugated goat α-mouse and Alexa488-conjugated goat α-rabbit anti-
554 bodies (ThermoFisher; 1:500). Images were captured on a Zeiss LSM-5 PASCAL laser scanning
555 confocal microscope. Pearson Correlation Coefficients were calculated (*n*=4) with Fiji software
556 and images were processed using Adobe Photoshop and Fiji software.

557

558 *L. pneumophila* intracellular growth curves

559 To quantify *L. pneumophila* intracellular replication, macrophages were seeded in 24-well tissue
560 culture plates and infected in triplicates at an MOI of 1 the next day. BMDMs were seeded at
561 $2.5x10^5$ in seeding media (RPMI, 10% HIFBS, 7.5% L929 cell supernatant), THP-1 cells were
562 seeded at $5x10^5$ and differentiated with 100 nM PMA in RPMI 10% HIFBS for three days. Cells
563 were washed with PBS and incubated in the absence of PMA for one day prior to infection. Stable
564 RAW 264.7 cells were seeded at $2.5x10^5$ in DMEM 2.5%HIFBS. MH-S cells were cultured in RPMI
565 10% HIFBS and seeded at $2.5x10^5$. At 1 h post-infection, cells were washed 3x with PBS followed
566 by addition of fresh media. Macrophages were lysed in sterile water and colony forming units
567 (CFU) were enumerated at the indicated time points as described (Ngwaga et al., 2019). Where
568 indicated, 25 ng mL^{-1} rTNF (Gibco), 5 ng mL^{-1} rIFN-γ (Gibco), 10 μM H_2O_2 (VWR), 10 nM bafilo-
569 mycin A1 (BAF; ApexBio), or 1 μM MCC950 (ApexBio) were added at the time of infection and

570 maintained throughout. DMSO was used as a vehicle control where indicated. Fold replication
571 was quantified by normalizing colony forming units to internalized bacteria at 1h post-infection.
572
573 Enzyme-linked immunosorbent assay (ELISA)
574 To quantify TNF secretion, 2.5 x 10^5 BMDMs were seeded in 24-well tissue culture plates and
575 infected with the indicated *L. pneumophila* strains at an MOI of 10. After 1 h of infection, cells
576 were washed with PBS, and media were replaced. Supernatants were at 8 h post-infection and
577 used fresh or stored at -20˚C for up to 1 week and TNF was quantified using mouse TNF-
578 α ELISA MAX kit following manufacturer's instructions. Absorbance at 450 nm was quantified
579 on a BioTek Epoch2 microplate reader.
580
581 Quantification of cell death and metabolic activity
582 To quantify cell death, lactate dehydrogenase activity in cell supernatants was quantified. BMDMs
583 were seeded in triplicates at 2.5x10^5 in a 24-well tissue culture plate for 24 h and infected with the
584 indicated *L. pneumophila* strains at an MOI of 10 in 500 µL of seeding media (RPMP/10%
585 HIFBS/7.5% L929 cell supernatant) and incubated for the indicated times. Supernatants were
586 transferred to a 96-well plate and centrifuged at 200 r.c.f. for 10 min. LDH was quantified using
587 the CytoTox 96 Non-Radioactive Cytotoxicity Assay (Promega) according to manufacturer's in-
588 structions. Absorbance at 490 nm was quantified on a BioTek Epoch2 microplate reader and per-
589 cent cytotoxicity was calculated by normalizing absorbance values to cells treated with lysis buffer.
590 Where indicated, cells were primed with 1 µM PAM3CSK4 (Tocris) for 24 h prior to infection.
591 To quantify cellular metabolic activity, an MTT colorimetric assay was used. BMDMs were
592 seeded in a 96-well tissue culture plate at 1x10^5 and infected the next day with the indicated *L.*
593 *pneumophila* strains at an MOI of 10. Cells were treated with 10 ng mL-1 rTNF and/or 10 µM
594 staurosporine (Abcam), as indicated. Cells were assayed using the MTT Cell Proliferation Assay
595 Kit (Colorimetric; BioVision) at 2 h and 24 h post-infection according to manufacturer's

596 instructions. Absorbance at 590 nm was quantified on a BioTek Epoch2 microplate reader and
597 percent viability was calculated by normalizing absorbance values to uninfected cells (100% via-
598 bility).
599
600 Statistical analysis
601 Statistical analyses were performed with GraphPad Prism 9 software using either Students' *t*-test,
602 or two-way ANOVA, as indicated, with a 95% confidence interval, as indicated. Unless otherwise
603 indicated, data are presented as mean ± standard deviation (s.d.) and statistical analyses was per-
604 formed on samples in triplicates.
605
606 **Acknowledgements**
607 We thank Drs. Mary Weber, Kalyani Pyaram, and Philip Hardwidge for critical feedback on the
608 manuscript and Dr. Russell Vance for femurs from *Casp1*$^{-/-}$ mice and helpful discussions. We also
609 thank Andrew Haskell for assistance within blinded microscopic scoring of *L. pneumophila*-in-
610 fected cells. This work was funded by NIH/NIGMS P20GM130448 (to S.R.S.); Kansas State Uni-
611 versity Johnson Cancer Research Center Summer Stipend Award (to T.N.) and Faculty Expansion
612 Award (to S.R.S.); a Kansas-INBRE Postdoctoral Fellowship (P20GM103418 to D.C.); Kansas-
613 INBRE Semester Scholar Award (P20GM103418 to A.G.S.); and startup funds from Kansas State
614 University (to S.R.S.).
615

616
617 **REFERENCES**
618

619 Archer, K.A., and Roy, C.R. (2006). MyD88-Dependent Responses Involving Toll-Like Receptor
620 2 Are Important for Protection and Clearance of Legionella pneumophila in a Mouse Model of
621 Legionnaires' Disease. Infect Immun *74*, 3325 3333. https://doi.org/10.1128/iai.02049-05.

622 Asrat, S., Dugan, A.S., and Isberg, R.R. (2014). The frustrated host response to Legionella pneu-
623 mophila is bypassed by MyD88-dependent translation of pro-inflammatory cytokines. Plos
624 Pathog *10*, e1004229. https://doi.org/10.1371/journal.ppat.1004229.

625 Bandyopadhyay, P., and Steinman, H.M. (2000). Catalase-Peroxidases of Legionella pneumoph-
626 ila: Cloning of the katA Gene and Studies of KatA Function. J Bacteriol *182*, 6679–6686.
627 https://doi.org/10.1128/jb.182.23.6679-6686.2000.

628 Bandyopadhyay, P., Byrne, B., Chan, Y., Swanson, M.S., and Steinman, H.M. (2003). Legionella
629 pneumophila Catalase-Peroxidases Are Required for Proper Trafficking and Growth in Primary
630 Macrophages. Infect Immun *71*, 4526–4535. https://doi.org/10.1128/iai.71.8.4526-4535.2003.

631 Bartel, P.L., and Fields, S. (1995). [16] Analyzing protein-protein interactions using two-hybrid
632 system. Methods Enzymol *254*, 241–263. https://doi.org/10.1016/0076-6879(95)54018-0.

633 Bergsbaken, T., Fink, S.L., and Cookson, B.T. (2009). Pyroptosis: host cell death and inflamma-
634 tion. Nat Rev Microbiol *7*, 99 109. https://doi.org/10.1038/nrmicro2070.

635 Byrne, B.G., Dubuisson, J.-F., Joshi, A.D., Persson, J.J., and Swanson, M.S. (2013). Inflam-
636 masome Components Coordinate Autophagy and Pyroptosis as Macrophage Responses to Infec-
637 tion. Mbio *4*, e00620-12. https://doi.org/10.1128/mbio.00620-12.

638 Case, C.L., and Roy, C.R. (2013). Analyzing caspase-1 activation during Legionella pneumophila
639 infection in macrophages. Methods in Molecular Biology (Clifton, NJ) *954*, 479 491.
640 https://doi.org/10.1007/978-1-62703-161-5_29.

641 Chauhan, D., and Shames, S.R. (2021). Pathogenicity and Virulence of Legionella: Intracellular
642 replication and host response. Virulence *12*, 1122–1144.
643 https://doi.org/10.1080/21505594.2021.1903199.

644 Choy, A., Dancourt, J., Mugo, B., O'Connor, T.J., Isberg, R.R., Melia, T.J., and Roy, C.R. (2012).
645 The Legionella effector RavZ inhibits host autophagy through irreversible Atg8 deconjugation.
646 Science *338*, 1072 1076. https://doi.org/10.1126/science.1227026.

647 Dikic, I. (2016). Proteasomal and Autophagy Degradation Systems. Annu Rev Biochem *86*, 1–
648 32. https://doi.org/10.1146/annurev-biochem-061516-044908.

649 Fabunmi, R.P., Wigley, W.C., Thomas, P.J., and DeMartino, G.N. (2001). Interferon gamma reg-
650 ulates accumulation of the proteasome activator PA28 and immunoproteasomes at nuclear PML
651 bodies. J Cell Sci *114*, 29–36. .

652 Feeley, J.C., Gibson, R.J., Gorman, G.W., Langford, N.C., Rasheed, J.K., Mackel, D.C., and
653 Baine, W.B. (1979). Charcoal-yeast extract agar: primary isolation medium for Legionella pneu-
654 mophila. Journal of Clinical Microbiology *10*, 437 441. .

655 Feuvre, R.A.L., Brough, D., Iwakura, Y., Takeda, K., and Rothwell, N.J. (2002). Priming of Mac-
656 rophages with Lipopolysaccharide Potentiates P2X7-mediated Cell Death via a Caspase-1-de-
657 pendent Mechanism, Independently of Cytokine Production*. J Biol Chem *277*, 3210–3218.
658 https://doi.org/10.1074/jbc.m104388200.

659 Fischer, N.L., Naseer, N., Shin, S., and Brodsky, I.E. (2019). Effector-triggered immunity and
660 pathogen sensing in metazoans. Nat Microbiol *5*, 14–26. https://doi.org/10.1038/s41564-019-
661 0623-2.

662 Flynn, K.J., and Swanson, M.S. (2014). Integrative Conjugative Element ICE-βox Confers Oxida-
663 tive Stress Resistance to Legionella pneumophila In Vitro and in Macrophages. Mbio *5*, e01091-
664 14. https://doi.org/10.1128/mbio.01091-14.

665 Fontana, M.F., Banga, S., Barry, K.C., Shen, X., Tan, Y., Luo, Z.-Q., and Vance, R.E. (2011). Se-
666 creted bacterial effectors that inhibit host protein synthesis are critical for induction of the in-
667 nate immune response to virulent Legionella pneumophila. Plos Pathog *7*, e1001289.
668 https://doi.org/10.1371/journal.ppat.1001289.

669 Formstecher, E., Aresta, S., Collura, V., Hamburger, A., Meil, A., Trehin, A., Reverdy, C., Betin,
670 V., Maire, S., Brun, C., et al. (2005). Protein interaction mapping: A Drosophila case study. Ge-
671 nome Res *15*, 376–384. https://doi.org/10.1101/gr.2659105.

672 Fromont-Racine, M., Rain, J.-C., and Legrain, P. (1997). Toward a functional analysis of the
673 yeast genome through exhaustive two-hybrid screens. Nat Genet *16*, 277–282.
674 https://doi.org/10.1038/ng0797-277.

675 Ghosh, S., and O'Connor, T.J. (2017). Beyond Paralogs: The Multiple Layers of Redundancy in
676 Bacterial Pathogenesis. Front Cell Infect Mi *7*, 467. https://doi.org/10.3389/fcimb.2017.00467.

677 Gomez-Valero, L., Rusniok, C., Carson, D., Mondino, S., Pérez-Cobas, A.E., Rolando, M.,
678 Pasricha, S., Reuter, S., Demirtas, J., Crumbach, J., et al. (2019). More than 18,000 effectors in
679 the Legionella genus genome provide multiple, independent combinations for replication in hu-
680 man cells. Proc National Acad Sci *116*, 2265 2273. https://doi.org/10.1073/pnas.1808016116.

681 Graaf, N. de, Helden, M.J.G. van, Textoris-Taube, K., Chiba, T., Topham, D.J., Kloetzel, P.-M.,
682 Zaiss, D.M.W., and Sijts, A.J.A.M. (2011). PA28 and the proteasome immunosubunits play a
683 central and independent role in the production of MHC class I-binding peptides in vivo. Eur J
684 Immunol *41*, 926–935. https://doi.org/10.1002/eji.201041040.

685 Hallermalm, K., Seki, K., Wei, C., Castelli, C., Rivoltini, L., Kiessling, R., and Levitskaya, J.
686 (2001). Tumor necrosis factor-α induces coordinated changes in major histocompatibility class I
687 presentation pathway, resulting in increased stability of class I complexes at the cell surface.
688 Blood *98*, 1108–1115. https://doi.org/10.1182/blood.v98.4.1108.

689 Harada, T., Miyake, M., and Imai, Y. (2007). Evasion of Legionella pneumophila from the Bacte-
690 ricidal System by Reactive Oxygen Species (ROS) in Macrophages. Microbiol Immunol *51*, 1161–
691 1170. https://doi.org/10.1111/j.1348-0421.2007.tb04011.x.

692 Hugoson, E., Guliaev, A., Ammunét, T., and Guy, L. (2022). Host-adaptation in Legionellales is
693 1.9 Ga, coincident with eukaryogenesis. Mol Biol Evol https://doi.org/10.1093/mol-
694 bev/msac037.

695 Ingmundson, A., Delprato, A., Lambright, D.G., and Roy, C.R. (2007). Legionella pneumophila
696 proteins that regulate Rab1 membrane cycling. Nature *450*, 365–369.
697 https://doi.org/10.1038/nature06336.

698 Khweek, A.A., Caution, K., Akhter, A., Abdulrahman, B.A., Tazi, M., Hassan, H., Majumdar, N.,
699 Doran, A., Guirado, E., Schlesinger, L.S., et al. (2013). A bacterial protein promotes the recogni-
700 tion of the Legionella pneumophila vacuole by autophagy. Eur J Immunol *43,* 1333 1344.
701 https://doi.org/10.1002/eji.201242835.

702 Lesne, J., Locard-Paulet, M., Parra, J., Zivković, D., Menneteau, T., Bousquet, M.-P., Burlet-
703 Schiltz, O., and Marcoux, J. (2020). Conformational maps of human 20S proteasomes reveal
704 PA28- and immuno-dependent inter-ring crosstalks. Nat Commun *11*, 6140.
705 https://doi.org/10.1038/s41467-020-19934-z.

706 Li, J., Powell, S.R., and Wang, X. (2010). Enhancement of proteasome function by PA28α
707 overexpression protects against oxidative stress. Faseb J Official Publ Fed Am Soc Exp Biology
708 *25*, 883–893. https://doi.org/10.1096/fj.10-160895.

709 Liu, X., Boyer, M.A., Holmgren, A.M., and Shin, S. (2020). Legionella-Infected Macrophages
710 Engage the Alveolar Epithelium to Metabolically Reprogram Myeloid Cells and Promote Anti-
711 bacterial Inflammation. Cell Host Microbe https://doi.org/10.1016/j.chom.2020.07.019.

712 MacMicking, J.D. (2012). Interferon-inducible effector mechanisms in cell-autonomous immun-
713 ity. Nat Rev Immunol *12*, 367 382. https://doi.org/10.1038/nri3210.

714 Marra, A., Blander, S.J., Horwitz, M.A., and Shuman, H.A. (1992). Identification of a Legionella
715 pneumophila locus required for intracellular multiplication in human macrophages. Proc Na-
716 tional Acad Sci *89*, 9607–9611. https://doi.org/10.1073/pnas.89.20.9607.

717 Matsumoto, N., and Nakanishi-Matsui, M. (2019). Proton pumping V-ATPase inhibitor bafilo-
718 mycin A1 affects Rab7 lysosomal localization and abolishes anterograde trafficking of osteoclast
719 secretory lysosomes. Biochem Bioph Res Co *510*, 421–426.
720 https://doi.org/10.1016/j.bbrc.2019.01.118.

721 Mitchell*, G., Chen*, C., and Portnoy, D.A. (2016). Strategies Used by Bacteria to Grow in Mac-
722 rophages. Microbiol Spectr *4*. https://doi.org/10.1128/microbiolspec.mchd-0012-2015.

723 Molofsky, A.B., Byrne, B.G., Whitfield, N.N., Madigan, C.A., Fuse, E.T., Tateda, K., and Swan-
724 son, M.S. (2006). Cytosolic recognition of flagellin by mouse macrophages restricts Legionella
725 pneumophila infection. J Exp Medicine *203*, 1093 1104. https://doi.org/10.1084/jem.20051659.

726 Mott, J.D., Pramanik, B.C., Moomaw, C.R., Afendis, S.J., DeMartino, G.N., and Slaughter, C.A.
727 (1994). PA28, an activator of the 20 S proteasome, is composed of two nonidentical but homolo-
728 gous subunits. J Biological Chem *269*, 31466–31471. .

729 Naujoks, J., Tabeling, C., Dill, B.D., Hoffmann, C., Brown, A.S., Kunze, M., Kempa, S., Peter, A.,
730 Mollenkopf, H.-J., Dorhoi, A., et al. (2016). IFNs Modify the Proteome of Legionella-Containing
731 Vacuoles and Restrict Infection Via IRG1-Derived Itaconic Acid. Plos Pathog *12*, e1005408.
732 https://doi.org/10.1371/journal.ppat.1005408.

733 Ngwaga, T., Hydock, A.J., Ganesan, S., and Shames, S.R. (2019). Potentiation of Cytokine-Medi-
734 ated Restriction of Legionella Intracellular Replication by a Dot/Icm-Translocated Effector. J
735 Bacteriol *201*, 13. https://doi.org/10.1128/jb.00755-18.

736 Ngwaga, T., Chauhan, D., and Shames, S.R. (2021). Mechanisms of Effector-Mediated Immunity
737 Revealed by the Accidental Human Pathogen Legionella pneumophila. Front Cell Infect Mi *10*,
738 593823. https://doi.org/10.3389/fcimb.2020.593823.

739 Orvedahl, A., McAllaster, M.R., Sansone, A., Dunlap, B.F., Desai, C., Wang, Y.-T., Balce, D.R.,
740 Luke, C.J., Lee, S., Orchard, R.C., et al. (2019). Autophagy genes in myeloid cells counteract
741 IFNγ-induced TNF-mediated cell death and fatal TNF-induced shock. Proc National Acad Sci
742 *116*, 16497–16506. https://doi.org/10.1073/pnas.1822157116.

743 Pandey, U.B., Nie, Z., Batlevi, Y., McCray, B.A., Ritson, G.P., Nedelsky, N.B., Schwartz, S.L., Di-
744 Prospero, N.A., Knight, M.A., Schuldiner, O., et al. (2007). HDAC6 rescues neurodegeneration
745 and provides an essential link between autophagy and the UPS. Nature *447*, 860–864.
746 https://doi.org/10.1038/nature05853.

747 Park, J.M., Ghosh, S., and O'Connor, T.J. (2020). Combinatorial selection in amoebal hosts
748 drives the evolution of the human pathogen Legionella pneumophila. Nat Microbiol 1–11.
749 https://doi.org/10.1038/s41564-019-0663-7.

750 Pickering, A.M., Koop, A.L., Teoh, C.Y., Ermak, G., Grune, T., and Davies, K.J.A. (2010). The im-
751 munoproteasome, the 20S proteasome and the PA28αβ proteasome regulator are oxidative-
752 stress-adaptive proteolytic complexes. Biochem J *432*, 585–594.
753 https://doi.org/10.1042/bj20100878.

754 Preckel, T., Fung-Leung, W.-P., Cai, Z., Vitiello, A., Salter-Cid, L., Winqvist, O., Wolfe, T.G.,
755 Herrath, M.V., Angulo, A., Ghazal, P., et al. (1999). Impaired Immunoproteasome Assembly and
756 Immune Responses in PA28−/− Mice. Science *286*, 2162–2165. https://doi.org/10.1126/sci-
757 ence.286.5447.2162.

758 Price, C.T.D., Hanford, H.E., Vashishta, A., Ozanic, M., Santic, M., Uriarte, S., and Kwaik, Y.A.
759 (2021). Dot/Icm-Dependent Restriction of Legionella pneumophila within Neutrophils. Mbio
760 *12*, e01008-21. https://doi.org/10.1128/mbio.01008-21.

761 Ren, T., Zamboni, D.S., Roy, C.R., Dietrich, W.F., and Vance, R.E. (2006). Flagellin-deficient Le-
762 gionella mutants evade caspase-1- and Naip5-mediated macrophage immunity. Plos Pathog *2*,
763 e18. https://doi.org/10.1371/journal.ppat.0020018.

764 Rolando, M., Escoll, P., Nora, T., Botti, J., Boitez, V., Bedia, C., Daniels, C., Abraham, G., Sto-
765 gios, P.J., Skarina, T., et al. (2016a). Legionella pneumophila S1P-lyase targets host sphingolipid
766 metabolism and restrains autophagy. Proc National Acad Sci *113*, 1901 1906.
767 https://doi.org/10.1073/pnas.1522067113.

768 Rolando, M., Escoll, P., and Buchrieser, C. (2016b). Legionella pneumophila restrains autophagy
769 by modulating the host's sphingolipid metabolism. Autophagy *12*, 1053–1054.
770 https://doi.org/10.1080/15548627.2016.1166325.

771 Roy, C.R., Berger, K.H., and Isberg, R.R. (1998). Legionella pneumophila DotA protein is re-
772 quired for early phagosome trafficking decisions that occur within minutes of bacterial uptake.
773 Mol Microbiol *28*, 663–674. https://doi.org/10.1046/j.1365-2958.1998.00841.x.

774 Saito, A., Rolfe, R.D., Edelstein, P.H., and Finegold, S.M. (1981). Comparison of liquid growth
775 media for Legionella pneumophila. Journal of Clinical Microbiology *14*, 623 627. .

776 Seifert, U., Bialy, L.P., Ebstein, F., Bech-Otschir, D., Voigt, A., Schröter, F., Prozorovski, T.,
777 Lange, N., Steffen, J., Rieger, M., et al. (2010). Immunoproteasomes Preserve Protein Homeo-
778 stasis upon Interferon-Induced Oxidative Stress. Cell *142*, 613–624.
779 https://doi.org/10.1016/j.cell.2010.07.036.

780 Shames, S.R., Deng, W., Guttman, J.A., Hoog, C.L. de, Li, Y., Hardwidge, P.R., Sham, H.P., Val-
781 lance, B.A., Foster, L.J., and Finlay, B.B. (2010). The pathogenic E. coli type III effector EspZ in-
782 teracts with host CD98 and facilitates host cell prosurvival signalling. Cell Microbiol *12*, 1322
783 1339. https://doi.org/10.1111/j.1462-5822.2010.01470.x.

784 Shames, S.R., Liu, L., Havey, J.C., Schofield, W.B., Goodman, A.L., and Roy, C.R. (2017). Multi-
785 ple Legionella pneumophila effector virulence phenotypes revealed through high-throughput
786 analysis of targeted mutant libraries. Proc National Acad Sci *63*, 201708553.
787 https://doi.org/10.1073/pnas.1708553114.

788 Shin, J.N., Fattah, E.A., Bhattacharya, A., Ko, S., and Eissa, N.T. (2013). Inflammasome Activa-
789 tion by Altered Proteostasis*. J Biol Chem *288*, 35886–35895.
790 https://doi.org/10.1074/jbc.m113.514919.

791 Soza, A., Knuehl, C., Groettrup, M., Henklein, P., Tanaka, K., and Kloetzel, P.-M. (1997). Expres-
792 sion and subcellular localization of mouse 20S proteasome activator complex PA28. Febs Lett
793 *413*, 27–34. https://doi.org/10.1016/s0014-5793(97)00864-8.

794 Sturgill-Koszycki, S., and Swanson, M.S. (2000). Legionella pneumophila Replication Vacuoles
795 Mature into Acidic, Endocytic Organelles. J Exp Medicine *192*, 1261–1272.
796 https://doi.org/10.1084/jem.192.9.1261.

797 Swanson, M.S., and Isberg, R.R. (1995). Association of Legionella pneumophila with the macro-
798 phage endoplasmic reticulum. Infection and Immunity *63*, 3609 3620. .

799 West, A.P., Brodsky, I.E., Rahner, C., Woo, D.K., Erdjument-Bromage, H., Tempst, P., Walsh,
800 M.C., Choi, Y., Shadel, G.S., and Ghosh, S. (2011). TLR signalling augments macrophage bacteri-
801 cidal activity through mitochondrial ROS. Nature *472*, 476 480. https://doi.org/10.1038/na-
802 ture09973.

803 Wilk, S., Chen, W.-E., and Magnusson, R.P. (2000). Properties of the Beta Subunit of the Pro-
804 teasome Activator PA28 (11S REG). Arch Biochem Biophys *384*, 174–180.
805 https://doi.org/10.1006/abbi.2000.2112.

806 Xie, S.C., Metcalfe, R.D., Hanssen, E., Yang, T., Gillett, D.L., Leis, A.P., Morton, C.J., Kuiper,
807 M.J., Parker, M.W., Spillman, N.J., et al. (2019). The structure of the PA28-20S proteasome
808 complex from Plasmodium falciparum and implications for proteostasis. Nat Microbiol *4*, 1990–
809 2000. https://doi.org/10.1038/s41564-019-0524-4.

810 Ziltener, P., Reinheckel, T., and Oxenius, A. (2016). Neutrophil and Alveolar Macrophage-Medi-
811 ated Innate Immune Control of Legionella pneumophila Lung Infection via TNF and ROS. Plos
812 Pathog *12*, e1005591. https://doi.org/10.1371/journal.ppat.1005591.

813

814

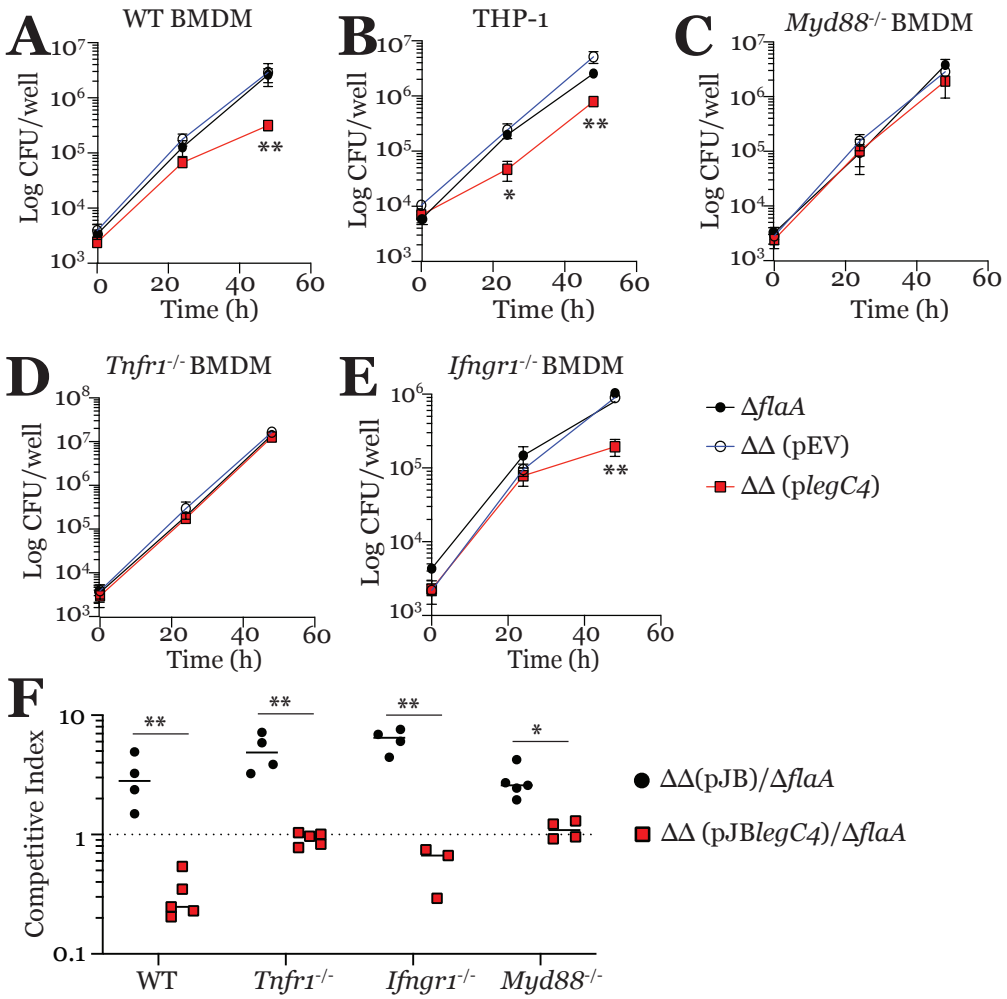

Figure 1. LegC4 attenuates *L. pneumophila* replication within cytokine-activated macrophages and the mouse lung. Growth of indicated *L. pneumophila* strains within **(A)** WT BMDMs, **(B)** THP-1 cells, **(C)** *Myd88*$^{-/-}$ BMDMs, **(D)** *Tnfr1*$^{-/-}$ BMDMs, or **(E)** *Ifngr1*$^{-/-}$ BMDMs over 48 h. Plasmid expression of *legC4* was induced with 1 mM IPTG. Macrophages were infected in triplicates and data are presented as mean ± standard deviation (s.d.). Asterisks denote statistical significance by Student's *t*-test (**P*<0.05, ***P*<0.01) and data are representative of three independent experiments. ΔΔ: Δ*flaA*Δ*legC4*. **(F)** Competitive index (CI) of *L. pneumophila* ΔΔ (pJB*legC4*) or Δ*flaA*Δ*legC4* (pJB) versus *L. pneumophila* Δ*flaA* in the lungs of the indicated at 48 h post-infection. Mice were infected with a total of 5x10^{6} bacteria in a 1:1 mixture and CI was calculated as

826 described (see Materials and Methods). Each symbol represents an individual animal and aster-
827 isks denote statistical significance by Two-way ANOVA (**P<0.001, *P<0.05). Data are repre-
828 sentative of three independent experiments. ΔΔ: Δ*flaA*Δ*legC4*
829

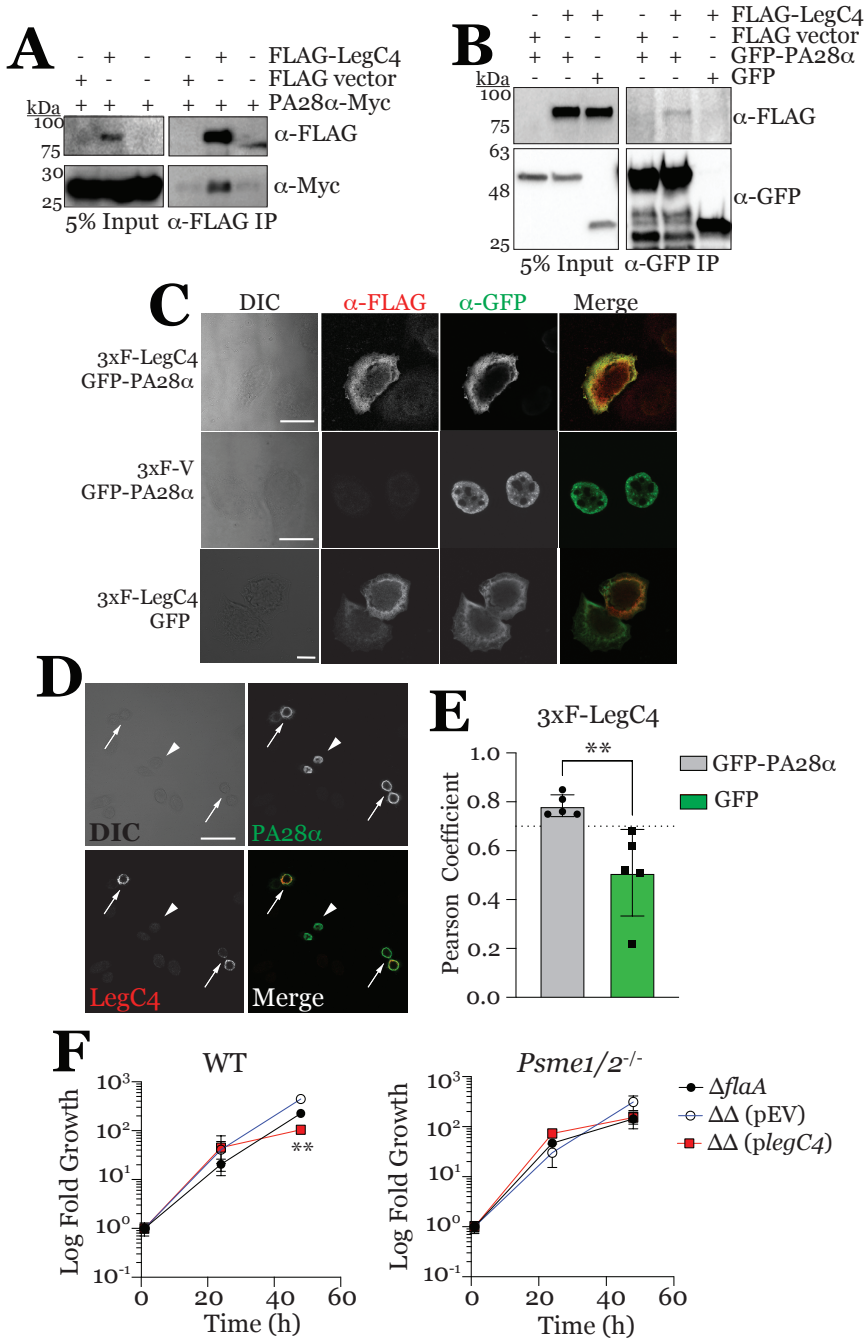

Figure 2. LegC4 interacts with PA28α and PA28αβ is important for LegC4-mediated restriction. **(A)** Western blot of co-immunoprecipitation of PA28α-Myc with 3xFLAG-LegC4 on a-FLAG conjugated magnetic beads (**A**) or 3xFLAG-LegC4 with GFP-PA28α on a-GFP-conjugated magnetic beads **(B)** from lysates of transfected HEK 293T cells. Data are representative of two independent

836 experiments. **(C)** Confocal microscopy to image HeLa cells co-transfected to ectopically produce
837 3xFLAG-LegC4 (red) and either GFP-PA28α or GFP (green). Scale bar represents 10 μm. (D) Con-
838 focal micrograph of HeLa cells producing GFP-PA28α (arrowhead) or GFP-PA28α and 3xFLAG-
839 LegC4 (arrows). Scale bar represents 50 μm. **(E)** Pearson Correlation Coefficients for cells pro-
840 ducing 3xFLAG-LegC4 and either GFP-PA28α or GFP alone (n=4). PCC ≥ 0.7 (dashed line) indi-
841 cates a high confidence association. Asterisks denote statistical significance by Students' *t*-test
842 (**P<0.01). Data shown are representative of two independent experiments. **(F)** Fold replication
843 of indicated *L. pneumophila* strains within WT (left) or *Psme1/2*$^{-/-}$ (right) or BMDMs. Plasmid
844 expression of *legC4* was induced with 1 mM IPTG. Macrophages were infected in triplicates and
845 data are presented as mean ± s.d. Asterisks denote statistical significance by Students' *t*-test
846 (**P<0.01). Data shown are representative of three independent experiments. ΔΔ: Δ*flaA*Δ*legC4*
847

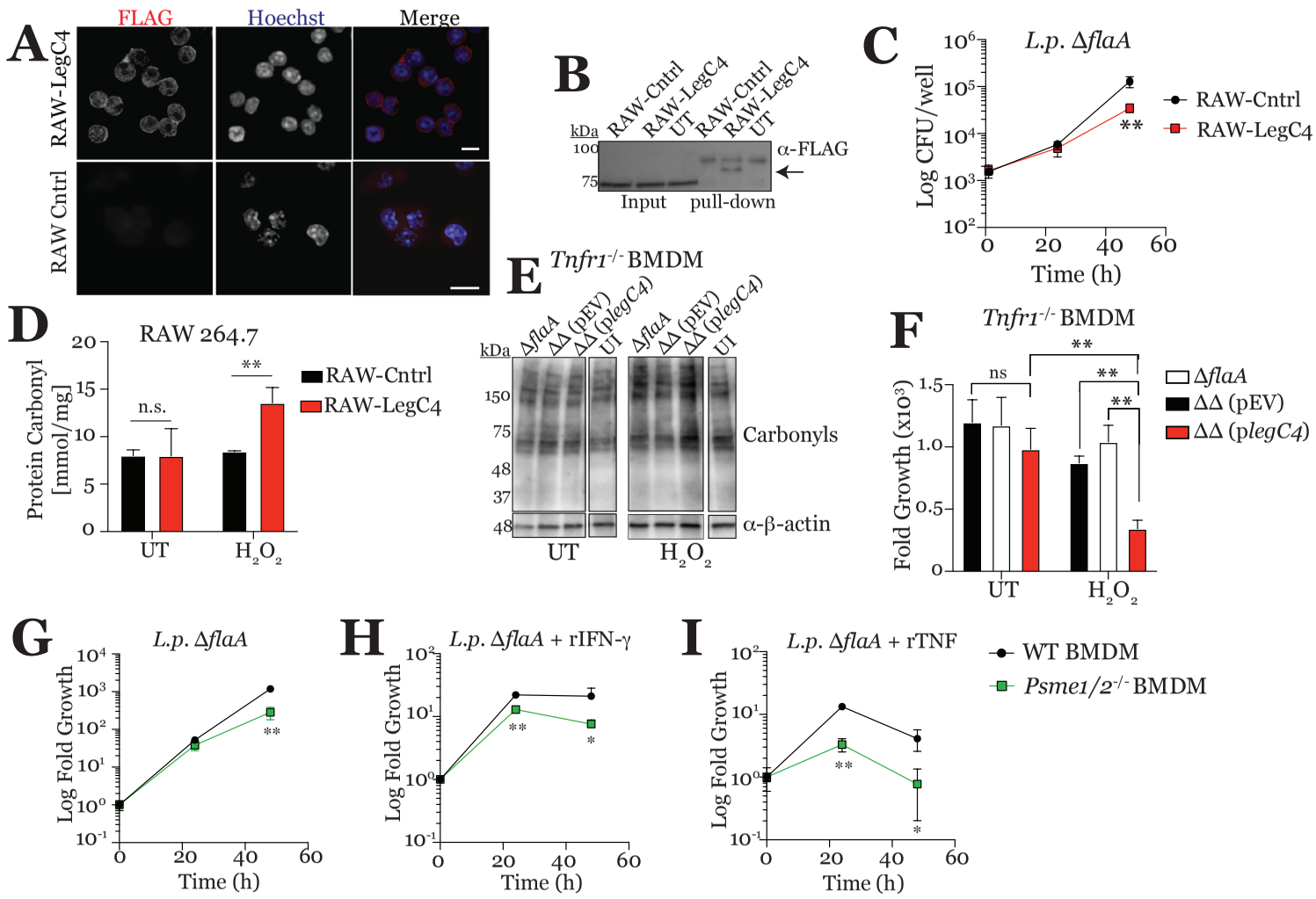
A
FLAG
Hoechst
Merge
RAW-LegC4
RAW Cntrl
B
RAW-Cntrl
RAW-LegC4
UT
RAW-Cntrl
RAW-LegC4
UT
kDa
100
75
α-FLAG
Input
pull-down
C
L.p. ΔflaA
Log CFU/well
Time (h)
RAW-Cntrl
RAW-LegC4
**
D
RAW 264.7
Protein Carbonyl [mmol/mg]
n.s.
**
RAW-Cntrl
RAW-LegC4
UT
H2O2
E
Tnfr1-/- BMDM
kDa
ΔflaA
ΔΔ (pEV)
ΔΔ (plegC4)
UI
150
75
48
37
48
Carbonyls
α-β-actin
UT
H2O2
F
Tnfr1-/- BMDM
Fold Growth (x10³)
ns
**
ΔflaA
ΔΔ (pEV)
ΔΔ (plegC4)
UT
H2O2
G
L.p. ΔflaA
Log Fold Growth
Time (h)
**
H
L.p. ΔflaA + rIFN-γ
Log Fold Growth
Time (h)
**
*
I
L.p. ΔflaA + rTNF
Log Fold Growth
Time (h)
**
*
WT BMDM
Psme1/2-/- BMDM

851 **Figure 3.** LegC4 impairs resolution of oxidative stress, which is sufficient for *L. pneumophila*
852 restriction. **(A)** Confocal microscopy to visualize 3xFLAG-LegC4 (red) production by stable
853 RAW 264.7 cells (RAW-LegC4). Mock transfected cells (RAW-Cntrl) were used as a control and
854 nuclei were imaged with Hoechst. Scale bar represents 10 μm. **(B)** Western blot analysis of
855 3xFLAG-LegC4 immunoprecipitated from lysates of RAW-LegC4, RAW-Cntrl or untransfected
856 (UT) RAW cells using α-FLAG-conjugated beads. Arrow indicates 3xFLAG-LegC4 (~84 kDa).
857 **(C)** Growth of *L. pneumophila* Δ*flaA* within RAW-LegC4 and -Cntrl cells. Data shown repre-
858 sentative of three experiments. **(D)** ELISA quantification of protein carbonyls in lysates of
859 RAW-LegC4 and -Cntrl cells incubated for 24 h in the presence or absence of 10 μM H_2O_2. Data
860 are representative of two independent experiments. **(E)** Western blot for protein carbonyls and
861 actin (loading control) in lysates of *Tnfr1*$^{-/-}$ BMDMs infected for 4 h with the indicated strains at
862 an MOI of 50. ΔΔ: Δ*flaA*Δ*legC4*; plasmid expression of *legC4* was induced with 1 mM IPTG.
863 Data are representative of three independent experiments. **(F)** Fold replication of *L. pneumoph-*
864 *ila* strains at 48 h post-infection within *Tnfr1*$^{-/-}$ BMDMs in the presence or absence of 10 μM
865 H_2O_2 as indicated. Plasmid expression of *legC4* was induced with 1 mM IPTG. Data are repre-
866 sentative of three independent experiments. **(G-I)** Fold replication of *L. pneumophila* (*L.p.*)
867 Δ*flaA* within WT or *Psme1/2*$^{-/-}$ BMDMs untreated **(G)** or treated with **(H)** 5 ng mL^{-1} rIFN-γ or
868 **(I)** 25 ng mL^{-1} rTNF. Macrophages were infected in triplicates and data are presented as mean ±
869 s.d. Asterisks denote statistical significance by Students' *t*-test (**P<0.01). All quantitative data
870 are presented as mean ± s.d. from samples in triplicates. Asterisks denote statistical significance
871 by Students' *t*-test (**P<0.01; ns., not significant). Data are representative of two independent
872 experiments. ΔΔ: Δ*flaA*Δ*legC4*
873

874

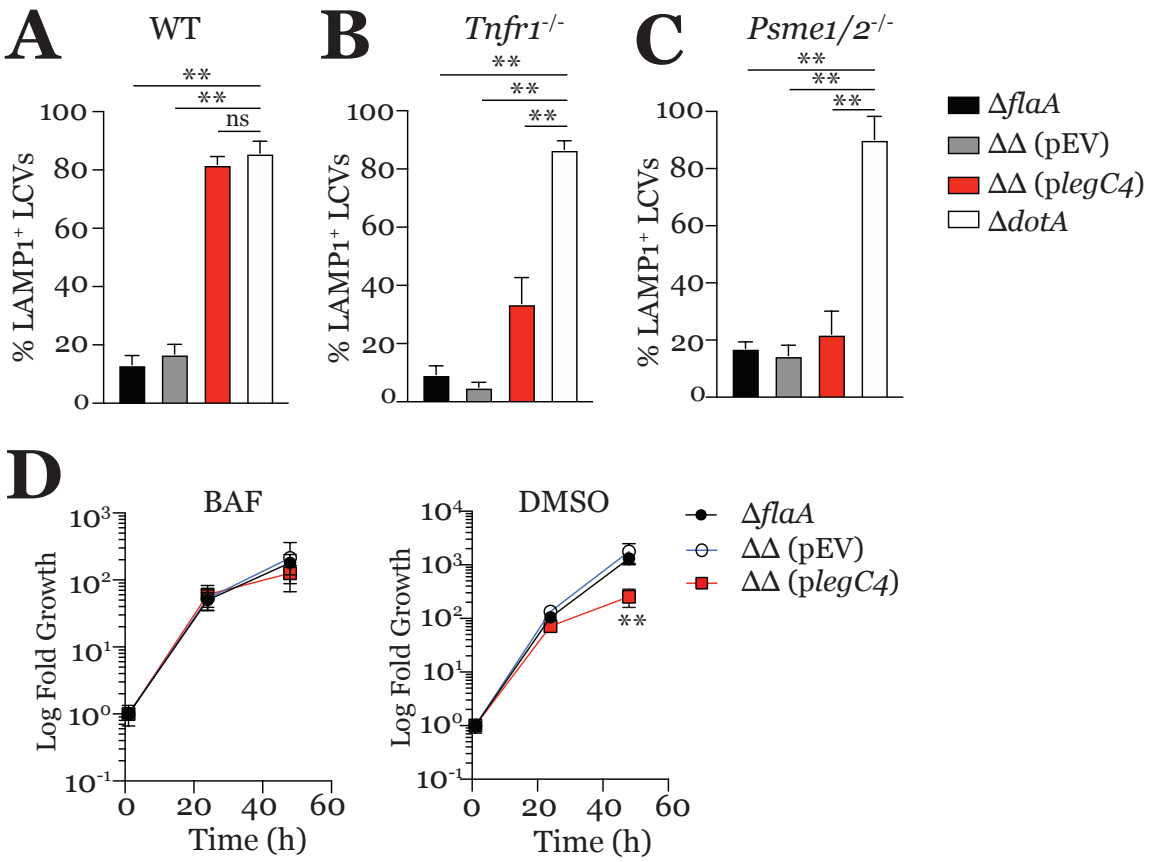

875

876 **Figure 4**. LegC4 induces lysosomal fusion with LCVs. Blinded immunofluorescence scoring of
877 LAMP1 localization to LCVs within BMDMs derived from WT **(A)**, *Tnfr1*$^{-/-}$ **(B)**, or *Psme1/2*$^{-/-}$ **(C)**
878 mice after 9 h of infection. Macrophages were infected in triplicates (n=300 per strain; moi of 30)
879 and LAMP1 localization to LCVs was quantified over two independent experiments. Plasmid ex-
880 pression of *legC4* was induced with 1 mM IPTG. Asterisks denote statistical significance by Stu-
881 dents' *t*-test (**P<0.01; ns, not significant). **(D)** Growth of *L. pneumophila* strains within WT
882 BMDMs treated with 10 nM bafilomycin A1 (BAF) (left panel) or DMSO (vehicle control; right
883 panel). Plasmid expression of *legC4* was induced with 1 mM IPTG. Asterisks denote statistical
884 significance by Students' *t*-test (**P<0.01). All data are presented as mean ± s.d. of samples in
885 triplicates and are representative of three independent experiments. ΔΔ: Δ*flaA*Δ*legC4*

886